Spectroscopy and Directed Transport of Topological Solitons in Crystals of Trapped Ions

J. Brox, P. Kiefer, M. Bujak, and T. Schaetz*
Albert-Ludwigs-Universität Freiburg, Physikalisches Institut, Hermann-Herder-Strasse 3, 79104 Freiburg, Germany

H. Landa†
LPTMS, CNRS, Université Paris-Sud, Université Paris-Saclay, 91405 Orsay, France

(Received 12 May 2017; published 12 October 2017)

We study experimentally and theoretically discrete solitons in crystalline structures consisting of several tens of laser-cooled ions confined in a radio frequency trap. Resonantly exciting localized, spectrally gapped vibrational modes of the soliton, a nonlinear mechanism leads to a nonequilibrium steady state of the continuously cooled crystal. We find that the propagation and the escape of the soliton out of its quasi-one-dimensional channel can be described as a thermal activation mechanism. We control the effective temperature of the soliton's collective coordinate by the amplitude of the external excitation. Furthermore, the global trapping potential permits controlling the soliton dynamics and realizing directed transport depending on its topological charge.

DOI: 10.1103/PhysRevLett.119.153602

Molecular scale transport is of considerable interest [1–3]. Biological "molecular motors" are submicron machines that consume nondirectional energy enabling directed transport, typically restricted to a one-dimensional (1D) "track." At these scales a fundamental question concerns the competition of the self-propelled motion with stochastic forces. Similarly, membrane channels, nanopores, and nanotubes can be modeled as 1D or quasi-1D systems with a cross section comparable to the size of the transported ion or molecule. Here, the entire channel forms the machine controlling the rate and direction of matter transport between two regions against a gradient (e.g., electrochemical), acting in addition to the noise. A prominent model for such dynamics is the Brownian ratchet, or Brownian motor [4], where the basic assumptions are the vanishing of all mean forces and the existence of significant noise. To allow the emergence of nonvanishing (mean) currents, the breaking of a symmetry is required—either spatial or temporal, stochastic or spontaneous.

A natural generalization of the single-particle ratchet to a many-body, nonlinear setting can be achieved with solitons, nonperturbative solutions that manifest a collective particlelike behavior [5,6] (Fig. 1). However, solitons are not point particles and have some extension in space, in addition to carrying internal degrees of freedom, e.g., oscillatory localized modes. These topologically protected excitations permit the transport of mass, energy, charge, spin, and other conserved quantities, in a broad range of optical, atomic, soft matter, and solid-state systems [7–30]. For soliton ratchets, the internal modes play a crucial role in the dynamics [31–38], since they can couple to external excitations and, due to nonlinearities, induce a motion of the soliton. In lattice systems, an effective pinning potential for discrete solitons appears—the Peierls-Nabarro (PN) potential. An *ab initio* theory of Brownian discrete soliton ratchets is hence nontrivial and currently limited to 1D systems with a continuum limit [39]. Experimentally accessible are continuum soliton ratchets in Josephson junction devices [40–44], while proposals exist for optical [45], atomic [46], and solid-state systems [47].

In this Letter, we demonstrate experimental spectroscopy of internal vibrational modes of a micrometer-scale discrete soliton. Furthermore, we show that, in the presence of

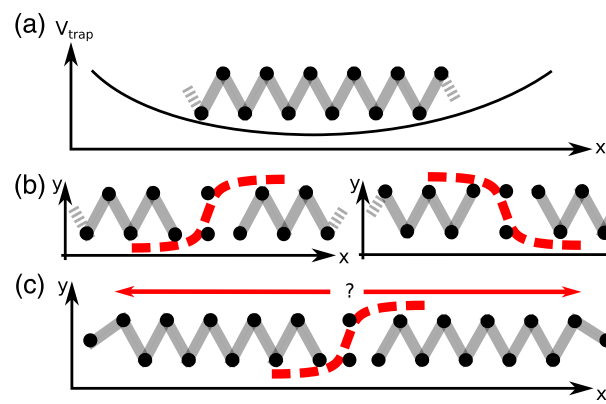

FIG. 1. Schematic depiction of discrete solitons and their propagation in a trapped Coulomb crystal. (a) The self-assembled crystal features reflection symmetry, and its energy minimum comes in two degenerate configurations: the "zigzag" and its mirror image "$\overline{\text{zigzag}}$" (only one shown). (b) Realizing both configurations in one crystal requires an interface, a domain wall called a "kink" (left) or "$\overline{\text{kink}}$" (right), which is a discrete soliton, carrying a topological charge of ±1, illustrated with a dashed red line. (c) In this Letter, we ask whether a resonant global excitation of radial vibrational kink modes can be rectified by the soliton and exploited to conditionally propagate it to the right or left in a noisy environment.

damping and fluctuations, the discrete soliton can be directed towards one end of its channel at a rate conditional on its topological charge and controllable by global external potentials. This is achieved by rectifying a harmonic drive of high frequency that has a negligible effect in the absence of the soliton. Therefore, the presented mechanism could serve as a model for soliton-based transport of mass, charge, or other conserved quantities.

Trapped ions are well suited for studying fundamental concepts down to the quantum level, featuring unique control in the preparation, manipulation, and detection of electronic and motional degrees of freedom [48]. Isolated in ultrahigh vacuum, they can be laser cooled to micro-Kelvin temperatures and localized to the nanometer scale. The effective potential for an ion near the center of a radio frequency (rf) Paul trap is approximately harmonic in 3D, with characteristic trapping frequencies $\omega_{\{x,y,z\}}$. Considering multiple ions, the potential has to be supplemented by the mutual Coulomb interaction, and an ordered, self-assembled crystal is formed that can be scaled to a mesoscopic size of interest to investigate many-body physics [49]. Figure 1 shows schematically how, for appropriate trapping frequencies $\omega_x \ll \omega_y < \omega_z$, the doubly degenerate ground state of such a crystal takes a planar, inhomogeneous zigzag configuration (we denote the mirrored configuration by $\overline{\text{zigzag}}$). To realize both configurations in one crystal, a localized interface, a domain wall [e.g., the kink and $\overline{\text{kink}}$ shown in Fig. 1(b)], must form, with a higher energy and the properties of a topological soliton [50]. Such discrete solitons have been recently characterized theoretically [51,52] and manipulated experimentally [53–59] and are predicted in circular [50,60,61] and helical configurations [62,63]. In particular, they are proposed to permit quantum coherent manipulation of their internal modes [58,61,64] using the rich toolbox of quantum optics developed for trapped ions [65].

To describe the classical dynamics of discrete solitons, we start by considering the $3N$ normal modes of N trapped ions, assuming small oscillations around their equilibrium positions. We consider one representative realization with $N = 34$ Mg^+ atoms and experimentally determined trap frequencies $\omega_{\{x,y,z\}} = 2\pi \times (\{38.2, 232.3, 293.0\} \pm 0.1)$ kHz. For the zigzag and $\overline{\text{zigzag}}$ configuration, we find mode frequencies $\omega^{\text{zigzag}}_{\{1,\ldots,102\}}$ in the range $2\pi \times 38.2$ to $2\pi \times 328$ kHz, while, with a kink or a $\overline{\text{kink}}$, the additional nonlinearity broadens the range of $\omega^{\text{kink}}_{\{1,\ldots,102\}}$ to $2\pi \times 23.2$ to $2\pi \times 345$ kHz [66]. A distinct set of internal modes can be attributed to the kink and $\overline{\text{kink}}$.

In the experiment, we probe the internal modes of the discrete soliton, using a spectroscopic protocol consisting of four steps: (i) inducing a phase transition [49] from a gas of trapped ions to a Coulomb crystal by laser cooling, (ii) *in situ* imaging of the crystal to reveal the potential presence of the kink, (iii) excitation of the kink using a weak periodic drive, and (iv) detecting the configuration, analyzing the kink's response to the excitation.

In step (i), a kink is formed and stabilized [54,58] with near 0.5 probability. (ii) The crystallized ions scatter laser photons that are collected in a charge-coupled device (CCD) camera, resolving the ion-ion separation with submicrometer accuracy, allowing us to differentiate the crystal configurations. (iii) During an excitation of duration t_d, we modulate the peak voltage (U_{rf}) on the trap's rf electrodes applying a voltage $U_d \sin(\omega_d t)$ calibrated by the experimentally determined transfer function of the rf circuit. Defining the relative excitation depth $\epsilon = U_d/U_{\mathrm{rf}}$, the force acting on each ion is derivable from the potential $V_d \propto \epsilon \sin(\omega_d t)[y^2 - z^2]$. The constant of proportionality is set by the experimental setup, whereas ϵ remains fully controllable. The excitation acts uniformly on the ions' radial coordinates y and z, while they remain continuously Doppler cooled by an axial beam.

We run this sequence at least 100 times for each data point. Figure 2(a) shows two main resonances where the kink [Fig. 2(b)(I)] escapes from the crystal, when scanning ω_d up to the highest mode frequencies for $t_d = 85$ ms. These two resonances are close (within their width) to the frequencies of two internal modes of the kink, $\omega^{\text{kink}}_{97}$ and $\omega^{\text{kink}}_{100}$, derived for $\epsilon \to 0$. The reduced peak amplitude for $\omega^{\text{kink}}_{97}$ results from a smaller projection of its eigenvector components for each ion on the radial direction. To shed light on the mechanism leading to the disappearance of the kink at resonance, we image the kink during the driving time t_d. With small ϵ and ω_d chosen at a resonance, we find an axially blurred trace [Fig. 2(b)(II)]. We identify this as an induced excitation of the lowest-frequency kink mode, ω^{kink}_1, a localized shear mode of the two opposing ion chains oscillating out of phase and axially translating the soliton. Increasing ϵ leads to the dynamics imaged in Fig. 2(b)(III), demonstrating that due to the radial drive the kink reaches the axial edge of the crystal and escapes, while the crystal remains intact.

Molecular dynamics (MD) simulations allow further insight. In the limit of vanishing damping and kinetic energy, the individual localized mode resonant with ω_d is excited, and, on a slower time scale comparable with $1/\omega^{\text{kink}}_1 \approx 50$ μs, the energy leaks via nonlinear coupling to the rest of the modes. As the kink oscillations increase and extend over a few lattice sites, we must consider the laser cooling. Here, the dynamics of a single ion at the Doppler-cooling limit along the x axis can be modeled as a Brownian harmonic oscillator [68–71]. The damping coefficient γ_x and diffusion coefficient D_x are determined by the experimental parameters and obey a fluctuation-dissipation relation $D_x = \gamma_x k_B T_x/m$. The temperature T_x is of the order of the Doppler-cooling limit $T_D \approx 1$ mK and $\gamma_x/m \approx 2\pi \times 0.3$ kHz. Similar equations hold for the radial coordinates, with γ_y, $\gamma_z \ll \gamma_x$. Adding these Langevin dynamics to the MD simulations including the trap and

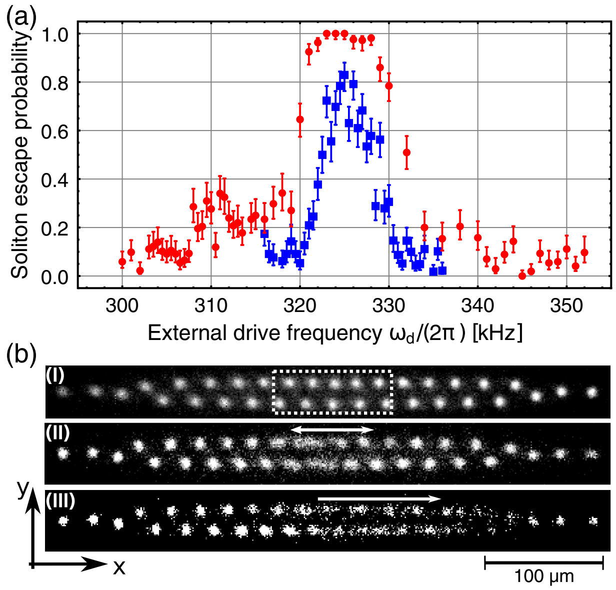

FIG. 2. Spectroscopy and directed escape of a discrete soliton. (a) Spectroscopically resolving kink modes via its complete escape from the crystal. With a periodic excitation of amplitude $\epsilon = 1.45 \times 10^{-3}$ (blue squares), we resolve a resonance at $\omega_d = 2\pi \times (325.3 \pm 0.2)$ kHz with a width of $2\pi \times (4.8 \pm 0.5)$ kHz. Strong excitation $\epsilon = 1.74 \times 10^{-3}$ (red disks) leads to saturation and an additional weaker resonance at $\omega_d = 2\pi \times (311 \pm 0.5)$ kHz of width $2\pi \times (4.4 \pm 1.8)$ kHz, in agreement with the numerically derived frequencies of internal modes (see the text for details). Error bars represent binomial statistics, and the offset level of 0.1 originates from background gas collisions at $\epsilon = 0$, leading to melting and recrystallization (background lifetime $\approx$3.2 s). (b) CCD images of the fluorescence of 34 ions confined in a Paul trap. (I) The center features the kink. (II) The modulation of the radial confinement resonantly excites a localized high-frequency vibrational kink mode, and its nonlinear coupling to other modes results in the axial blurring of the oscillating kink. (III) Escape of the soliton via the right-hand side is witnessed as the left half of the configuration remains unaffected, while on the right the two opposing ion chains have to "slide" atop each other. Because of the long exposure time of the camera, $t_{\mathrm{CCD}} = 150$ ms, both configurations are superimposed.

Coulomb interactions [58] and drive V_d defined above reveals that a nonequilibrium steady state is reached on a millisecond time scale. The characterization of this state is nontrivial [72]; however, the mixing of spatial directions by the quasi-2D crystal modes leads to an effective radial damping. The energy drawn from the radial drive by the kink's internal mode is transformed to heat in the crystal, balanced by axial laser cooling, and a mean kinetic energy in the crystal at the steady state, E_k, can be defined and is linearly related to ϵ. Using the measured experiment parameters, the shapes and positions of the resonances in Fig. 2 are reproduced quantitatively [72].

Next, we experimentally determine the survival probability of the kink as function of t_d, for different values of ϵ, with ω_d resonant at $\omega_{100}^{\mathrm{kink}}$. The survival probabilities [Fig. 3(a)] can be fitted by an exponential decay yielding a mean lifetime $\tau(\epsilon)$ that decreases with ϵ [Fig. 3(b)] [73]. This evidences a thermal activation mechanism for the kink's escape across a barrier. As it is known from numerical simulations that the PN potential in a trap becomes effectively harmonic [54], the value of the PN potential at the edges of the crystal defines the height of the barrier W. To model the dynamics of the escape, we use the numerically obtained positions of all ions to define an instantaneous collective kink coordinate [74], for the kink's axial position along the quasi-2D crystal featuring its 1D track. Following its time evolution, we find using the velocity autocorrelation function that it is overdamped. We fit the effective kink coordinate's friction coefficient $g(E_k)$, which depends on the mean kinetic energy stored in the crystal in the relevant temperature regime [72] originating from phonon scattering, finding $g(E_k) \propto E_k^{1/2}$. Then, assuming that the effective kink coordinate is subject to

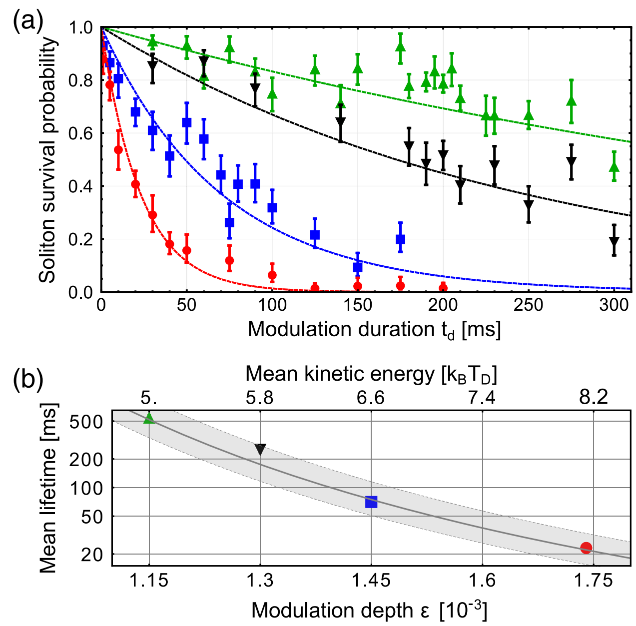

FIG. 3. Resonant drive of the radial kink mode leads to a thermally activated escape out of the PN potential. (a) Experimental survival probability of the soliton as a function of t_d for $\omega_d/(2\pi) = 327$ kHz and $\epsilon = 10^{-3} \times \{1.15$(green triangles), 1.30 (black inverted triangles), 1.45 (blue squares), and 1.74 (red disks)$\}$. Solid lines represent exponential fits yielding the corresponding lifetimes of the kink, $\tau(\epsilon) = \{(544 \pm 35), (248 \pm 16), (71 \pm 5), (23 \pm 2)\}$ ms, respectively. Error bars represent the 1σ confidence interval. The residual kink loss rate for $\epsilon = 0$ is subtracted based on a calibration measurements. (b) Lifetime of the kink in dependence on ϵ derived from panel (a), fitted with an overdamped Kramers' model [81] for symmetric confinement (see the text for details), indicated by the gray solid line. The experiment control parameter ϵ is numerically found to be linearly related to the mean kinetic energy of the ions, leading to an effective temperature. The gray shaded region represents 1σ uncertainty of the fit. We extract a related barrier height of $(26.5 \pm 1.0)k_B T_D$.

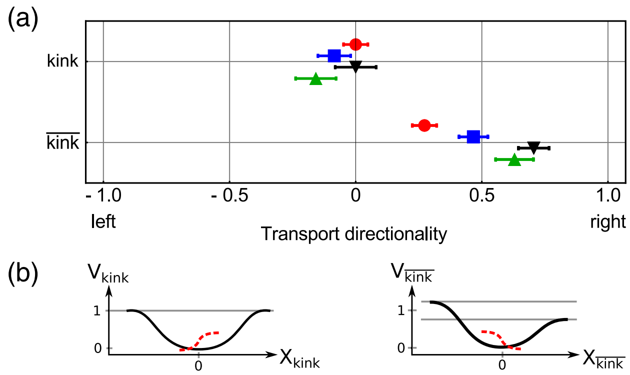

FIG. 4. Experimental transport directionality (TD) conditional on the topological charge: $\pm 1 \hat{=} \{\text{kink}, \overline{\text{kink}}\}$. (a) While the kink escapes with close to zero TD in the experiment, the $\overline{\text{kink}}$ reveals the broken symmetry tunable by nonlinear terms of the confining potential. Additionally, the TD depends on ϵ (symbols as in Fig. 3). Error bars give 1σ standard deviation. (b) The trapping potential for the soliton (schematically depicted) depends on its topological charge. It remains approximately left-right symmetric for the kink and is strongly asymmetric for the $\overline{\text{kink}}$. The trap depth for the whole Coulomb crystal amounts to $10^4 \times V_{\text{kink}}$.

thermal noise at an effective temperature [77] defined by $k_B T/2 = E_k/(3N)$, we apply Kramers' model in the overdamped limit [81,82] to describe the motion of the soliton [83,84]. The predicted mean lifetime of the Brownian particle obeys $\tau \propto g(T) e^{W/(k_B T)}$. The details of the PN potential are contained in the omitted proportionality constant, with only the barrier height W entering, averaged over the kink and $\overline{\text{kink}}$ and both directions. Based on the experimentally determined $\tau(\epsilon)$ [Fig. 3(b)], we find the value $W = (26.5 \pm 1.0) k_B T_D$.

Finally, we experimentally find a substantial directionality of the soliton transport dependent on its topological charge. We define the transport directionality (TD) as the normalized difference of probabilities to escape to the right and to the left. The TD of the kink remains near 0 for all ϵ [Fig. 4(a)], while for the $\overline{\text{kink}}$ we find a substantial bias to the right. The existence of a mean current implies a broken symmetry, and we extend the harmonic approximation of the trap potential by nonlinear terms [85] of third order along the x axis (L_x) and y axis (L_y) and also fourth order and mixed terms. We use the charge density (sensitive to these terms) as a sensor, by minimizing the weighted least-mean-square shift of the imaged ion positions and the measured frequencies ω_x and ω_y, from their numerically obtained values as a function of the nonlinear coefficients. In particular, we find $L_x > 0$, leading to a shift of the crystal towards $x < 0$, increasing the left-side PN barrier and decreasing it on the right. Similarly, $L_y < 0$ shifts the crystal to $y > 0$ and, due to the different radial densities of the kink and $\overline{\text{kink}}$, results in different PN barriers. The mean PN barrier numerically obtained is $W = 25.3 k_B T_D$, coinciding within error bars with the experimental value. An intricate interplay of the various global nonlinearity parameters explains the directionality measured in Fig. 4 [72], and we obtain an asymmetric shift of about $2 k_B T_D$ for W on the left and on the right. This differential shift is comparable to the increase of T with ϵ, reducing the soliton's sensitivity to the differences in W, as evidenced in Fig. 4. Thus, the directionality can be controlled via the nonlinear terms of the global trapping potential and U_d.

In conclusion, we find that the external radial drive can be tuned to pump energy through a kink mode, that is converted to heat, establishing power transfer in a nonequilibrium steady state. The nonlinearity of the trap potential affects the ions only perturbatively, and all mean forces vanish after the self-assembled crystal adjusts its configuration. The axial motion of the soliton can be described by integrating out all degrees of freedom leaving one effective coordinate, to which Kramers' model can be applied with an effective temperature. The directionality arises through the different W, conditioned on the topological charge, which is the manifestation of the underlying nonequilibrium conditions, and only the solitons can be transported. Typically, realizing a ratchet mechanism requires asymmetric gradients at the single-particle scale. We show how a large scale potential permits the robust control of the soliton transport, its direction, and rate.

These physical processes connect to a broad range of recently studied topics, nonequilibrium states [86–88], ratchets in granular chains [89], quantum ratchets [90,91], and ratchets with power law interaction [92], and studies with trapped ions on thermal activation [93], escape dynamics [94], and heat current formation [95–98]. The unique controllability of trapped ions further permits investigations of transport dynamics, e.g., concatenating crystals along a linear axis or studying ring configurations [50,61,99,100]. Ground state cooling of these internal modes has been proposed to enable accessing the quantum regime where the related phonons permit investigating coherent coupling and transport in mesoscopic, quasi-2D crystals [50,61]. Trapping of several discrete solitons has been realized [58,59] and a kink mode excitation demonstrated via intensity modulation of a single-ion focused laser beam [72], enabling the study of phonon-mediated energy transport in kink lattices.

Related work on local kink mode spectroscopy was performed in the context of friction and Aubry transitions [101].

H. L. thanks Martin Lenz, Ananyo Maitra, and Guglielmo Saggiorato for very fruitful discussions. H. L. acknowledges support by a Marie Curie Intra European Fellowship within the 7th European Community Framework Programme.

*tobias.schaetz@physik.uni-freiburg.de
†haggaila@gmail.com

[1] F. Jülicher, A. Ajdari, and J. Prost, Modeling molecular motors, Rev. Mod. Phys. 69, 1269 (1997).

[2] P. Hänggi and F. Marchesoni, Artificial Brownian motors: Controlling transport on the nanoscale, Rev. Mod. Phys. **81**, 387 (2009).

[3] R. Dean Astumian, S. Mukherjee, and A. Warshel, The physics and physical chemistry of molecular machines, ChemPhysChem **17**, 1719 (2016).

[4] S. Denisov, S. Flach, and P. Hänggi, Tunable transport with broken space-time symmetries, Phys. Rep. **538**, 77 (2014).

[5] R. Rajaraman, *Solitons and Instantons: An Introduction to Solitons and Instantons in Quantum Field Theory* (North-Holland Personal Library, North-Holland, Amsterdam, 1987).

[6] T. Dauxois and M. Peyrard, *Physics of Solitons* (Cambridge University Press, Cambridge, England, 2006).

[7] O. M. Braun and Y. S. Kivshar, *The Frenkel-Kontorova Model: Concepts, Methods, and Applications*, Texts and Monographs in Physics (Springer, New York, 2004).

[8] S. Flach and A. V. Gorbach, Discrete breathers—Advances in theory and applications, Phys. Rep. **467**, 1 (2008).

[9] M. Öster, M. Johansson, and A. Eriksson, Enhanced mobility of strongly localized modes in waveguide arrays by inversion of stability, Phys. Rev. E **67**, 056606 (2003).

[10] L. čo Hadžievski, A. Maluckov, M. Stepić, and D. Kip, Power Controlled Soliton Stability and Steering in Lattices with Saturable Nonlinearity, Phys. Rev. Lett. **93**, 033901 (2004).

[11] T. R. O. Melvin, A. R. Champneys, P. G. Kevrekidis, and J. Cuevas, Radiationless Traveling Waves in Saturable Nonlinear Schrödinger Lattices, Phys. Rev. Lett. **97**, 124101 (2006).

[12] R. A. Vicencio and M. Johansson, Discrete soliton mobility in two-dimensional waveguide arrays with saturable nonlinearity, Phys. Rev. E **73**, 046602 (2006).

[13] O. F. Oxtoby and I. V. Barashenkov, Moving solitons in the discrete nonlinear Schrödinger equation, Phys. Rev. E **76**, 036603 (2007).

[14] H. Susanto, P. G. Kevrekidis, R. Carretero-González, B. A. Malomed, and D. J. Frantzeskakis, Mobility of Discrete Solitons in Quadratically Nonlinear Media, Phys. Rev. Lett. **99**, 214103 (2007).

[15] U. Naether, R. A. Vicencio, and M. Johansson, Peierls-Nabarro energy surfaces and directional mobility of discrete solitons in two-dimensional saturable nonlinear Schrödinger lattices, Phys. Rev. E **83**, 036601 (2011).

[16] V. Ahufinger, A. Sanpera, P. Pedri, L. Santos, and M. Lewenstein, Creation and mobility of discrete solitons in Bose-Einstein condensates, Phys. Rev. A **69**, 053604 (2004).

[17] B. A Malomed, *Soliton Management in Periodic Systems* (Springer, New York, 2006).

[18] J. Abdullaev, D. Poletti, E. A. Ostrovskaya, and Y. S. Kivshar, Controlled Transport of Matter Waves in Two-Dimensional Optical Lattices, Phys. Rev. Lett. **105**, 090401 (2010).

[19] T. Fogarty, C. Cormick, H. Landa, V. M. Stojanović, E. Demler, and G. Morigi, Nanofriction in Cavity Quantum Electrodynamics, Phys. Rev. Lett. **115**, 233602 (2015).

[20] T. Fogarty, H. Landa, C. Cormick, and G. Morigi, Optomechanical many-body cooling to the ground state using frustration, Phys. Rev. A **94**, 023844 (2016).

[21] T. Sanchez, D. T. N. Chen, S. J. DeCamp, M. Heymann, and Z. Dogic, Spontaneous motion in hierarchically assembled active matter, Nature (London) **491**, 431 (2012).

[22] A. Ward, F. Hilitski, W. Schwenger, D. Welch, A. W. C. Lau, V. Vitelli, L. Mahadevan, and Z. Dogic, Solid friction between soft filaments, Nat. Mater. **14**, 583 (2015).

[23] T. Bohlein, J. Mikhael, and C. Bechinger, Observation of kinks and antikinks in colloidal monolayers driven across ordered surfaces, Nat. Mater. **11**, 126 (2012).

[24] A. Bylinskii, D. Gangloff, I. Counts, and V. Vuletić, Observation of Aubry-type transition in finite atom chains via friction, Nat. Mater. **15**, 717 (2016).

[25] M. V. Fistul, A. Wallraff, Yu. Koval, A. Lukashenko, B. A. Malomed, and A. V. Ustinov, Quantum Dissociation of a Vortex-Antivortex Pair in a Long Josephson Junction, Phys. Rev. Lett. **91**, 257004 (2003).

[26] D. Bedau, M. Kläui, S. Krzyk, U. Rüdiger, G. Faini, and L. Vila, Detection of Current-Induced Resonance of Geometrically Confined Domain Walls, Phys. Rev. Lett. **99**, 146601 (2007).

[27] T.-H. Kim and H. W. Yeom, Topological Solitons versus Nonsolitonic Phase Defects in a Quasi-One-Dimensional Charge-Density Wave, Phys. Rev. Lett. **109**, 246802 (2012).

[28] S. Brazovskii, C. Brun, Z.-Z. Wang, and P. Monceau, Scanning-Tunneling Microscope Imaging of Single-Electron Solitons in a Material with Incommensurate Charge-Density Waves, Phys. Rev. Lett. **108**, 096801 (2012).

[29] S. Roth and D. Carroll, *One-Dimensional Metals: Conjugated Polymers, Organic Crystals, Carbon Nanotubes*, 2nd ed. (Wiley-VCH, Weinheim, 2015), pp. 85–112, ISBN: 978-3-527-33557-2.

[30] P. Karpov and S. Brazovskii, Phase transitions in ensembles of solitons induced by an optical pumping or a strong electric field, Phys. Rev. B **94**, 125108 (2016).

[31] N. R. Quintero, A. Sánchez, and F. G. Mertens, Anomalous Resonance Phenomena of Solitary Waves with Internal Modes, Phys. Rev. Lett. **84**, 871 (2000).

[32] N. R. Quintero, A. Sánchez, and F. G. Mertens, Anomalies of ac driven solitary waves with internal modes: Nonparametric resonances induced by parametric forces, Phys. Rev. E **64**, 046601 (2001).

[33] M. Salerno and N. R. Quintero, Soliton ratchets, Phys. Rev. E **65**, 025602 (2002).

[34] S. Flach, Y. Zolotaryuk, A. E. Miroshnichenko, and M. V. Fistul, Broken Symmetries and Directed Collective Energy Transport in Spatially Extended Systems, Phys. Rev. Lett. **88**, 184101 (2002).

[35] L. Morales-Molina, N. R. Quintero, F. G. Mertens, and A. Sánchez, Internal Mode Mechanism for Collective Energy Transport in Extended Systems, Phys. Rev. Lett. **91**, 234102 (2003).

[36] C. R. Willis and M. Farzaneh, Soliton ratchets induced by excitation of internal modes, Phys. Rev. E **69**, 056612 (2004).

[37] P. J. Martínez and R. Chacón, Disorder Induced Control of Discrete Soliton Ratchets, Phys. Rev. Lett. **100**, 144101 (2008).

[38] J. Cuevas, B. Sánchez-Rey, and M. Salerno, Regular and chaotic transport of discrete solitons in asymmetric potentials, Phys. Rev. E **82**, 016604 (2010).

[39] B. Sánchez-Rey, N. R. Quintero, J. Cuevas-Maraver, and M. A. Alejo, Collective coordinates theory for discrete soliton ratchets in the sine-Gordon model, Phys. Rev. E **90**, 042922 (2014).

[40] E. Trías, J. J. Mazo, F. Falo, and T. P. Orlando, Depinning of kinks in a Josephson-junction ratchet array, Phys. Rev. E **61**, 2257 (2000).

[41] G. Carapella and G. Costabile, Ratchet Effect: Demonstration of a Relativistic Fluxon Diode, Phys. Rev. Lett. **87**, 077002 (2001).

[42] A. V. Ustinov, C. Coqui, A. Kemp, Y. Zolotaryuk, and M. Salerno, Ratchetlike Dynamics of Fluxons in Annular Josephson Junctions Driven by Biharmonic Microwave Fields, Phys. Rev. Lett. **93**, 087001 (2004).

[43] D. E. Shalóm and H. Pastoriza, Vortex Motion Rectification in Josephson Junction Arrays with a Ratchet Potential, Phys. Rev. Lett. **94**, 177001 (2005).

[44] M. Beck, E. Goldobin, M. Neuhaus, M. Siegel, R. Kleiner, and D. Koelle, High-Efficiency Deterministic Josephson Vortex Ratchet, Phys. Rev. Lett. **95**, 090603 (2005).

[45] A. V. Gorbach, S. Denisov, and S. Flach, Optical ratchets with discrete cavity solitons, Opt. Lett. **31**, 1702 (2006).

[46] D. Poletti, T. J. Alexander, E. A. Ostrovskaya, B. Li, and Y. S. Kivshar, Dynamics of Matter-Wave Solitons in a Ratchet Potential, Phys. Rev. Lett. **101**, 150403 (2008).

[47] Y. Zolotaryuk and M. M. Osmanov, Directed motion of domain walls in biaxial ferromagnets under the influence of periodic external magnetic fields, Eur. Phys. J. B **79**, 257 (2011).

[48] D. J. Wineland and W. M. Itano, Laser cooling of atoms, Phys. Rev. A **20**, 1521 (1979).

[49] R. Blümel, J. M. Chen, E. Peik, W. Quint, W. Schleich, Y. R. Shen, and H. Walther, Phase transitions of stored laser-cooled ions, Nature (London) **334**, 309 (1988).

[50] H. Landa, S. Marcovitch, A. Retzker, M. B. Plenio, and B. Reznik, Quantum Coherence of Discrete Kink Solitons in Ion Traps, Phys. Rev. Lett. **104**, 043004 (2010).

[51] A. del Campo, G. De Chiara, G. Morigi, M. B. Plenio, and A. Retzker, Structural Defects in Ion Chains by Quenching the External Potential: The Inhomogeneous Kibble-Zurek Mechanism, Phys. Rev. Lett. **105**, 075701 (2010).

[52] G. De Chiara, A. del Campo, G. Morigi, M. B. Plenio, and A. Retzker, Spontaneous nucleation of structural defects in inhomogeneous ion chains, New J. Phys. **12**, 115003 (2010).

[53] Ch. Schneider, D. Porras, and T. Schaetz, Experimental quantum simulations of many-body physics with trapped ions, Rep. Prog. Phys. **75**, 024401 (2012).

[54] M. Mielenz, H. Landa, J. Brox, S. Kahra, G. Leschhorn, M. Albert, B. Reznik, and T. Schaetz, Trapping of Topological-Structural Defects in Coulomb Crystals, Phys. Rev. Lett. **110**, 133004 (2013).

[55] K. Pyka, J. Keller, H. L. Partner, R. Nigmatullin, T. Burgermeister, D. M. Meier, K. Kuhlmann, A. Retzker, M. B. Plenio, W. H. Zurek, A. del Campo, and T. E. Mehlstubler, Topological defect formation and spontaneous symmetry breaking in ion Coulomb crystals, Nat. Commun. **4**, 2291 (2013).

[56] S. Ulm, J. Roßnagel, G. Jacob, C. Degünther, S. T. Dawkins, U. G. Poschinger, R. Nigmatullin, A. Retzker, M. B. Plenio, F. Schmidt-Kaler, and K. Singer, Observation of the Kibble-Zurek scaling law for defect formation in ion crystals, Nat. Commun. **4**, 8 (2013).

[57] S. Ejtemaee and P. C. Haljan, Spontaneous nucleation and dynamics of kink defects in zigzag arrays of trapped ions, Phys. Rev. A **87**, 051401 (2013).

[58] H. Landa, B. Reznik, J. Brox, M. Mielenz, and T. Schaetz, Structure, dynamics and bifurcations of discrete solitons in trapped ion crystals, New J. Phys. **15**, 093003 (2013).

[59] H. L. Partner, R. Nigmatullin, T. Burgermeister, K. Pyka, J. Keller, A. Retzker, M. B. Plenio, and T. E. Mehlstubler, Dynamics of topological defects in ion Coulomb crystals, New J. Phys. **15**, 103013 (2013).

[60] F. Cartarius, C. Cormick, and G. Morigi, Stability and dynamics of ion rings in linear multipole traps, Phys. Rev. A **87**, 013425 (2013).

[61] H. Landa, A. Retzker, T. Schaetz, and B. Reznik, Entanglement Generation Using Discrete Solitons in Coulomb Crystals, Phys. Rev. Lett. **113**, 053001 (2014).

[62] R. Nigmatullin, A. del Campo, G. De Chiara, G. Morigi, M. B. Plenio, and A. Retzker, Formation of helical ion chains, Phys. Rev. B **93**, 014106 (2016).

[63] A. V. Zampetaki, J. Stockhofe, and P. Schmelcher, Dynamics of nonlinear excitations of helically confined charges, Phys. Rev. E **92**, 042905 (2015).

[64] S. Marcovitch and B. Reznik, Entanglement of solitons in the Frenkel-Kontorova model, Phys. Rev. A **78**, 052303 (2008).

[65] D. J. Wineland, Superposition, entanglement, and raising Schrödinger's cat (Nobel Lecture), Angew. Chem. Int. Ed. **52**, 10179 (2013).

[66] We have verified that the dynamic nature of the Paul trap [67] leads in our setup to only small frequency shifts.

[67] H. Landa, M. Drewsen, B. Reznik, and A. Retzker, Modes of oscillation in radiofrequency Paul traps, New J. Phys. **14**, 093023 (2012).

[68] D. Leibfried, R. Blatt, C. Monroe, and D. Wineland, Quantum dynamics of single trapped ions, Rev. Mod. Phys. **75**, 281 (2003).

[69] M. Marciante, C. Champenois, A. Calisti, J. Pedregosa-Gutierrez, and M. Knoop, Ion dynamics in a linear radiofrequency trap with a single cooling laser, Phys. Rev. A **82**, 033406 (2010).

[70] J. Javanainen, Light-pressure cooling of trapped ions in three dimensions, Appl. Phys. **23**, 175 (1980).

[71] J. Javanainen and S. Stenholm, Laser cooling of trapped particles I: The heavy particle limit, Appl. Phys. **21**, 283 (1980).

[72] J. Brox, P. Kiefer, M. Bujak, T. Schaetz, and H. Landa (to be published).

[73] H. L. Partner, R. Nigmatullin, T. Burgermeister, J. Keller, K. Pyka, M. B. Plenio, A. Retzker, W. H. Zurek, A. del Campo, and T. E. Mehlstubler, Structural phase transitions and topological defects in ion Coulomb crystals, Physica B (Amsterdam) **460**, 114 (2015), Special Issue on Electronic Crystals.

[74] Collective coordinates of solitons are well described in Refs. [75,76]; we use the ansatz (A.3) of Ref. [59].

[75] R. Boesch, P. Stancioff, and C. R. Willis, Hamiltonian equations for multiple-collective-variable theories of

nonlinear Klein-Gordon equations: A projection-operator approach, Phys. Rev. B **38**, 6713 (1988).

[76] A. H. Castro Neto and A. O. Caldeira, Transport properties of solitons, Phys. Rev. E **48**, 4037 (1993).

[77] More elaborate models [78–80] could be considered in a second step.

[78] P. S. Burada and B. Lindner, Escape rate of an active Brownian particle over a potential barrier, Phys. Rev. E **85**, 032102 (2012).

[79] J. Schuecker, M. Diesmann, and M. Helias, Modulated escape from a metastable state driven by colored noise, Phys. Rev. E **92**, 052119 (2015).

[80] A. Geiseler, P. Hänggi, and G. Schmid, Kramers escape of a self-propelled particle, Eur. Phys. J. B **89**, 175 (2016).

[81] H. A. Kramers, Brownian motion in a field of force and the diffusion model of chemical reactions, Physica (Utrecht) **7**, 284 (1940).

[82] P. Hänggi, P. Talkner, and M. Borkovec, Reaction-rate theory: Fifty years after Kramers, Rev. Mod. Phys. **62**, 251 (1990).

[83] P. Grigolini, H.-L. Wu, and V. M. Kenkre, Brownian motion and finite-temperature effects in the discrete nonlinear Schrödinger equation: Analytic results for the nonadiabatic dimer, Phys. Rev. B **40**, 7045 (1989).

[84] P. S. Lomdahl and W. C. Kerr, Do Davydov Solitons Exist at 300 K?, Phys. Rev. Lett. **55**, 1235 (1985).

[85] N. Akerman, S. Kotler, Y. Glickman, Y. Dallal, A. Keselman, and R. Ozeri, Single-ion nonlinear mechanical oscillator, Phys. Rev. A **82**, 061402 (2010).

[86] E. Dieterich, J. Camunas-Soler, M. Ribezzi-Crivellari, U. Seifert, and F. Ritort, Single-molecule measurement of the effective temperature in non-equilibrium steady states, Nat. Phys. **11**, 971 (2015).

[87] A. Y. Grosberg and J.-F. Joanny, Nonequilibrium statistical mechanics of mixtures of particles in contact with different thermostats, Phys. Rev. E **92**, 032118 (2015).

[88] É. Fodor, C. Nardini, M. E. Cates, J. Tailleur, P. Visco, and F. van Wijland, How Far from Equilibrium Is Active Matter?, Phys. Rev. Lett. **117**, 038103 (2016).

[89] V. Berardi, J. Lydon, P. G. Kevrekidis, C. Daraio, and R. Carretero-González, Directed ratchet transport in granular chains, Phys. Rev. E **88**, 052202 (2013).

[90] L. Ermann and G. G. Carlo, Quantum parameter space of dissipative directed transport, Phys. Rev. E **91**, 010903 (2015).

[91] C. Grossert, M. Leder, S. Denisov, P. Hänggi, and M. Weitz, Experimental control of transport resonances in a coherent quantum rocking ratchet, Nat. Commun. **7**, 10440 (2016).

[92] B. Liebchen and P. Schmelcher, Interaction induced directed transport in ac-driven periodic potentials, New J. Phys. **17**, 083011 (2015).

[93] J. Liang and P. C. Haljan, Hopping of an impurity defect in ion crystals in linear traps, Phys. Rev. A **83**, 063401 (2011).

[94] C. Petri, S. Meyer, F. Lenz, and P. Schmelcher, Correlations and pair emission in the escape dynamics of ions from one-dimensional traps, New J. Phys. **13**, 023006 (2011).

[95] G.-Dar Lin and L. M. Duan, Equilibration and temperature distribution in a driven ion chain, New J. Phys. **13**, 075015 (2011).

[96] A. Bermúdez, M. Bruderer, and M. B. Plenio, Controlling and Measuring Quantum Transport of Heat in Trapped-Ion Crystals, Phys. Rev. Lett. **111**, 040601 (2013).

[97] M. Ramm, T. Pruttivarasin, and H. Häffner, Energy transport in trapped ion chains, New J. Phys. **16**, 063062 (2014).

[98] N. Freitas, E. A. Martinez, and J. Pablo Paz, Heat transport through ion crystals, Phys. Scr. **91**, 013007 (2016).

[99] U. Schramm, T. Schätz, and D. Habs, Bunched Crystalline Ion Beams, Phys. Rev. Lett. **87**, 184801 (2001).

[100] U. Schramm, T. Schätz, and D. Habs, Three-dimensional crystalline ion beams, Phys. Rev. E **66**, 036501 (2002).

[101] J. Kiethe, R. Nigmatullin, D. Kalincev, T. Schmirander, and T. E. Mehlstäubler, Probing nanofriction and Aubry-type signatures in a finite self-organized system, Nat. Commun. **8**, 15364 (2017).